ELASTOPLASTIC CRACK PROPAGATION

A.G. Atkins and Zhong Chen *

A closed-form algebraic solution for elastoplastic cracking in DCB testpieces has recently been derived(1): it is path-dependent and shows that while nlefm (Hencky total strain plasticity) well describes the onset of fracture from different starter crack lengths via a critical J_c or R, that theory is incapable of describing propagation. Experimental load-point displacements at identical crack lengths are all greater than nlefm predictions and moreover depend on the starting crack length. Our new analysis well predicts this behaviour. Normalised accumulated work (J_R curves) are all path-dependent, even within this one type of testpiece, leave alone between different types of specimen.

NLEFM Inadequate for Propagation in Ductile Fracture

Figure 1 demonstrates that the theory of non linear elastic fracture mechanics (nlefm), purporting to represent plasticity through Hencky total strain theory, fails to describe experimental crack propagation in ductile metals. The grooved double cantilever beam (DCB) testpiece is made of 6082–T6 aluminium alloy which approximates to an elastic-perfectly-plastic solid having E = 67.6 GPa and yield strength σ_o = 291 MPa. The end-loaded arms are such that they are partially plastic when cracking occurs. The testpiece with the shorter starter crack ℓ_o = 70 mm is loaded and the crack propagated until it has the length of the starter crack of the second specimen (140 mm). The second specimen is then loaded up to initiation. Figure 1 demonstrates that path-independence does not apply: the ≈ 25 mm displacement under load of the 70 mm crack propagated from the shorter starting crack is greater than the ≈ 14 mm of the testpiece with a 140 mm starter crack just at initiation. Furthermore, the unloaded displacements are also different (12 mm versus 1 mm).

* Department of Engineering, University of Reading, PO Box 225, Whiteknights, Reading, RG6 2AY. U.K.

The irreversible displacement associated with zones BCGFDB shown in Figure 2 is the origin of the greater displacement shown in Figure 1. In nlefm, zones BCGFDB would not exist in the first specimen after propagation because they would have disappeared on unloading during propagation and all their energy would have been released back into the system. But because in practical ductile bodies such zones represent mostly irreversible work, only some of the energy in these zones is recovered as (linear) elastic strain energy.

Elastoplastic Theory

Incorporation of the plastic zones left behind the moving crack front is crucial for proper elastoplastic propagation analyses in this and other cracked geometries. We have taken full account of those zones and present a closed-form algebraic solution for elastoplastic cracking in end-loaded beam testpieces, Atkins & Chen Zhong, (1). The crack-tip moment to produce fracture is given by

$$M(O) = bh^2\sigma_y \left\{1 - \frac{3}{4}(1-\phi)^2\right\} \tag{1}$$

where $\phi = ER/\sigma_o^2 h$, with E Young's modulus, R fracture toughness, σ_o yield strength, h beam depth and b beam thickness. Not only is this constant (cf. Gurney & Hunt, (2); Gurney & Ngan, (3); Calladine, (4) in small and large deformation globally elastic cases) but the elastoplastic M(O) is the same as that obtained from an nlefm solution to a related problem (Chang, DeVries & Williams, (5); Atkins & Mai, (6). What is different here is that the load-point-displacement w is greater in the elastoplastic case and is also path-dependent. Our new theory gives these path-dependent displacements.

Experiments and Results

Our present experiments include not only beams of different arm height giving different degrees of elastoplasticity, but also arms deep enough to give globally linear elastic behaviour.

Figure 3 shows that constant R loci of ca 22 kJ/m^2 predicted by our elastoplastic theory well-describe path-dependent propagation in DCB testpieces. The same R of 22 kJ/m^2 applies to the globally-elastic experiments in testpieces with deeper arm heights.

The same constant R locus given by the nlefm analysis runs through the initiation points but fails to describe the Pw co-ordinates during propagation.

Accumulated Work: J_R Plots

OBCH in Figure 4 is the accumulated work under load after crack advance $\Delta\ell$. Our elastoplastic theory predicts

$$\frac{U_{acc}}{(2b)\ell_o} = \frac{R}{\phi}\left\{\frac{160}{27(1-3\phi^2+6\phi)} - 1 - \frac{16(1-\phi)}{3(1-3\phi^2+6\phi)} + \frac{(1-\phi)}{3}\right\}$$

$$+ \frac{R(1-3\phi^2+6\phi)}{\phi}\left\{\frac{1}{6(1-\phi)} - \frac{(1-3\phi^2+6\phi)}{32}\right\}\frac{\Delta\ell}{\ell_o} \tag{2}$$

where ℓ_o is the starter crack length and $\Delta\ell$ the crack advance. This is a straight line relationship versus normalised crack advance $(\Delta\ell/\ell_o)$ with intercept and slope related to R by ϕ. When $\phi = 1/3$ we have global elasticity and then

$$U_{acc}/(2b)\ell_o = R/3 + (4R/3)(\Delta\ell/\ell_o) \qquad (3)$$

for linear elastic DCB testpieces, Atkins (7). The nlefm relation is similar to Equation (2) with the same intercept, but lower slope. The difference relates to the path-dependent load-point displacement and hence extra work of the elastoplastic case. Figure 5 shows that experiments and analysis agree well.

The plots are of course J_R-type curves. The intercepts depend on ϕ but all give R (i.e.J_c) $\approx$ 22 kJ/m^2. Clearly the slopes do not represent increased toughness, as sometimes said of J_R curves. We argue that the initiation value of R (J_c) controls propagation throughout. Furthermore the J_R-type plot cannot be a material property: here we show that there is history-dependence even within one type of testpiece, leave alone between different specimens. Note that we do not deny the possibility of R($\Delta\ell$) curves absorbing energy local to the crack path. We have avoided this complication in our experiments. What we do not do is couple the remote plastic flow in the arms with the work of fracture, which is the J_R approach.

References

(1) Atkins, A.G. & Chen Zhong, 1994. Submitted to Proc.R.Soc.A.
(2) Gurney, C & Hunt J, Proc. R.Soc. 1967. A 299, 508.
(3) Gurney, C & Ngan, K M, Proc. R. Soc. 1971. A325, 207.
(4) Calladine, C R, Proc. R. Soc. 1987. B229, 381.
(5) Chang, M D, Devries, K L & Williams, M L, J. Adhesion. 1972. 4, 221.
(6) Atkins, A G & Mai, Y W, Int.J.Fract. 1986. 30, 203.
(7) Atkins, A G, Int.J.Fract. 1991. 51, R45.

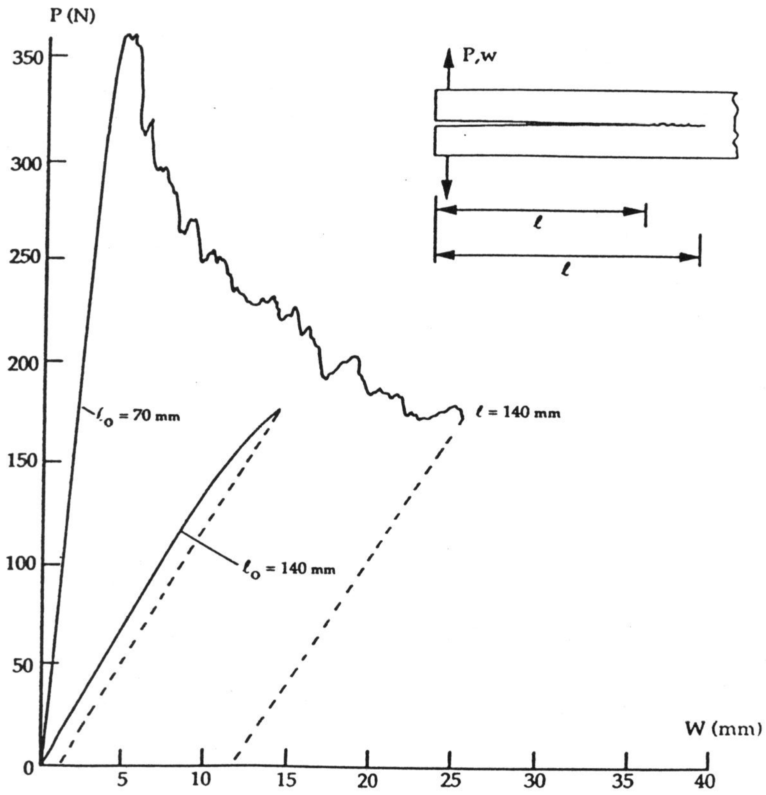

Fig.1. Path Dependence in load, displacement, crack length ($Pw\ell$) coordinates.

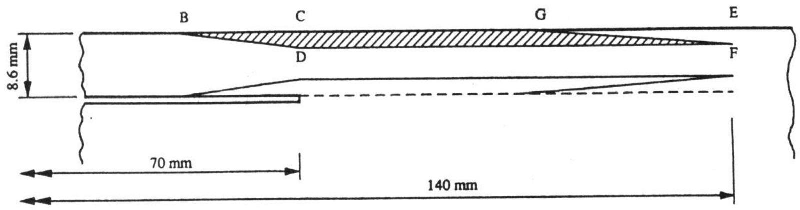

Fig.2. Plastic Zones. BCDB is the plastic zone at initiation in the testpiece with the 70 mm starter crack; after propagation to 140 mm, the zone is BEFDB. The zone at initiation in the 140 mm starter crack length testpiece is GEFG. In nlefm BCGFDB would disappear on propagation; in practical ductile materials only partial recovery takes place, leading to the different displacements in Figure 1.

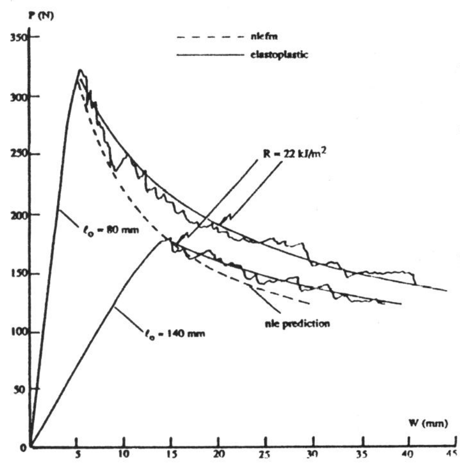

Fig.3a. Elastoplastic Experimental Results & Theoretical Predictions

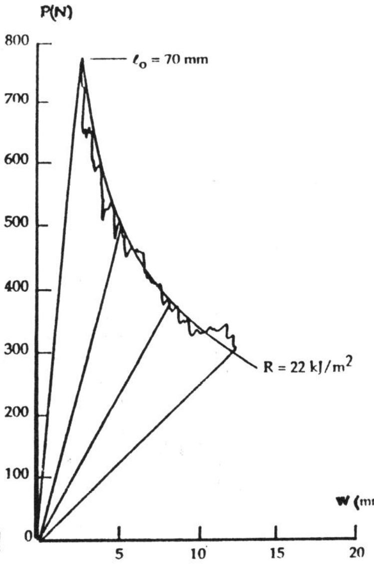

Fig.3b. Globally Elastic Experiments and Theoretical Predictions.

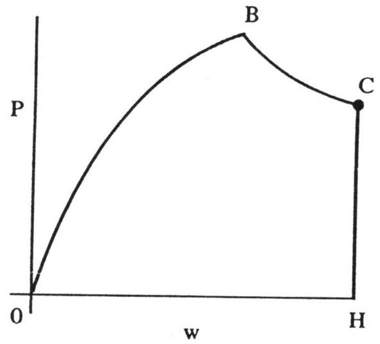

Fig.4. Accumulated Work U_{acc} during propagation. Work OBCH normalised by initial crack area plotted against $\Delta\ell$, or $\Delta\ell/\ell_o$, is a J_R-type curve.

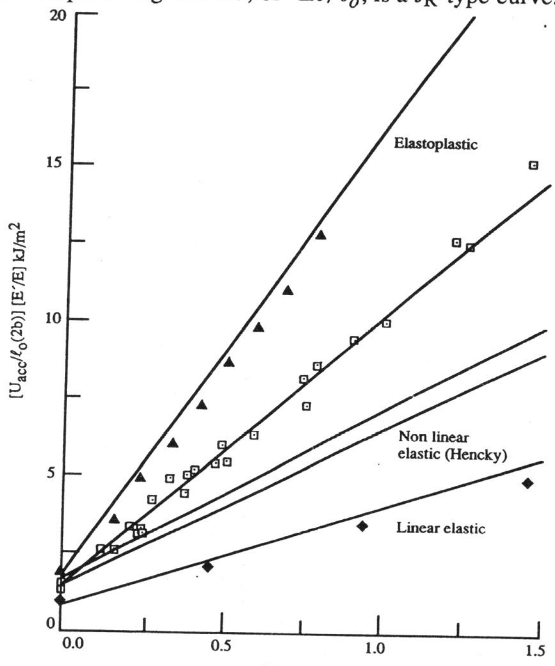

Fig.5. History-dependent J_R-type plots (E'/E factor to accommodate beam-on-elastic-foundation treatment of grooved crack path; E' foundation modulus). All plots correspond with constant R of 22 kJ/m^2 at initiation and throughout propagation.